Vol. 12(2): 366-384, May 2024 DOI: https://doi.org/10.23960/jsl.v12i2.889

Jurnal Sylva Lestari

P-ISSN: 2339-0913
E-ISSN: 2549-5747

Journal homepage: https://sylvalestari.fp.unila.ac.id

Full Length Research Article

The Effect of Synthetic and Commercial Nano-Magnetite on the Electromagnetic Absorbance Behavior of Magnetic Wood

Istie Sekartining Rahayu[1,*], Aqila Alya Nabila Sabarna[1], Irma Wahyuningtyas[2], Rohmat Ismail[3], Esti Prihatini[1], Wayan Darmawan[1], Gilang Dwi Laksono[1], Irsan Alipraja[1]

[1] Department of Forest Products, Faculty of Forestry and Environment, IPB University, Bogor, Indonesia
[2] Department of Forest Product Processing, Faculty of Forest Product Technology, Samarinda State Agricultural Polytechnic, Samarinda, Indonesia
[3] Department of Chemistry, Faculty of Mathematics and Natural Sciences, IPB University, Bogor, Indonesia
[*] Corresponding Author. E-mail address: istiesr@apps.ipb.ac.id

ARTICLE HISTORY:

Received: 16 January 2024
Peer review completed: 18 March 2024
Received in revised form: 28 March 2024
Accepted: 4 April 2024

KEYWORDS:

Fe_3O_4
Impregnation
Nano-magnetite
Sengon wood
Shielding materials

ABSTRACT

Magnetic wood with good electromagnetic wave absorption properties was prepared by comparing synthetic and commercial nano-magnetite (Fe_3O_4-NP) as sengon (*Falcataria moluccana*) wood impregnation solution. The co-precipitation method produced a synthetic nano-magnetite with NH_4OH as a weak base precursor. Meanwhile, the commercial one was purchased from a supplier. Three levels of nano-magnetite concentration (1%, 2.5%, and 5%) were dispersed in deionized water. The impregnation process was done by applying a vacuum of 0.5 bar for 120 minutes, followed by a pressure of 1 bar for 120 minutes. The results showed that the commercial nano-magnetite caused more improvements in weight percent gain, density, and hardness than the synthetic nano-magnetic, although they were insignificantly different. There was also a reduction in brightness with the overall color change being categorized into other colors because the color became darker with increasing nano-magnetite concentration in both woods. The absorbance capacity of the synthetic nano-magnetite-treated wood was larger than the commercial nano-magnetite-treated wood. This synthetic nano-magnetite-treated wood had been optimally treated at a 5% concentration, making it suitable for use as electromagnetic wave shielding material because it can absorb almost 100% electromagnetic waves.

1. Introduction

Wood modification has become a hot issue among researchers in recent decades as it can improve the performance of fast-growing wood to address the timber needs in Indonesia (Hadiyane et al. 2018). Wood materials support green building construction as a new alternative to traditional polymer composites owing to their lower environmental impacts (La Mantia and Morreale 2011). Many people also use this because they are interested in its durability and aesthetic superiority. Several previous studies have developed fast-growing wood modifications through acetylation, furfurylation (Hadi et al. 2020), impregnation (Hartono et al. 2016), chemical modification (Teng et al. 2018), and thermal modification (Hidayat et al. 2024; Suri et al. 2023). In addition to improving the intrinsic properties of wood, the modification process also allows the wood to

produce new properties and makes wood multifunctional (Sandberg et al. 2017). Therefore, it can expand its application and attract many consumers to use wood daily.

Sengon wood (*Falcataria moluccana*) is a fast-growing wood species widespread because of its abundance and ease of cultivation in community forests (Istikorini et al. 2022; Sopacua et al. 2021). Sengon wood has disadvantages, such as low density, strength, durability, specific gravity, and dimensional stability (Martawijaya et al. 2005). The high juvenility in sengon wood causes it to have low quality and is currently only used as insulating boards, plywood, carpentry wood, and crates (Darmawan et al. 2015). Thus, sengon wood is suitable as an experimental material for this study. Sengon wood will be converted into one of the most promising materials in the future, namely magnetic wood, through the impregnation process using nano-magnetite. This modification process is appropriate for increasing the use of sengon wood to become more valuable and multifunctional.

Magnetic wood is modified wood with high dimensional stability, durability, magnetically attracted, heat performance, and absorption of electromagnetic waves emitted by electronic devices (Dong et al. 2016; Trey et al. 2014). This wood can be prepared in several ways, such as wood coating, mixing sawdust and magnetic powder, or impregnation by immersing wood in magnetic fluids (Oka and Fujita 1999). Previously, Rahayu et al. (2022) succeeded in the fabrication of magnetic wood using nano-magnetite from the co-precipitation method, resulting in high physical and magnetic properties of sengon wood (*F. moluccana*) and jabon wood (*A. cadamba*). On the other hand, Laksono et al. (2023) and Wahyuningtyas et al. (2022) also synthesized magnetic wood using commercial nano-magnetite purchased from a supplier. These studies developed wood magnetic properties. Therefore, the modified wood has paramagnetic properties and was classified as a soft magnetic material. There is also an ex-situ impregnation method, which can be done easily and quickly and requires low costs (Prihatini et al. 2022).

As previously mentioned by Fadia et al. (2023a), using nano-magnetite synthesized via the co-precipitation method is believed to improve the wood's weight gain by more than 100% and reduce water absorption. Dong et al. (2016) also stated that poplar wood, which was magnetized by the co-precipitation method and continued with in situ polymerization, produced nano-magnetite with an average size of 16 nm, and much of it was deposited in the lumen cell, thereby reducing collapse in the wood. Merk et al. (2014) also revealed that the magnetic wood obtained by the co-precipitation method was highly susceptible to magnetic fields. Based on these characteristics, the application of synthetic nano-magnetite seems more effective in increasing wood quality and producing new material functions compared to commercial nano-magnetite uses that have a high possibility of agglomeration and clogging the wood pores, so it blocks the solution penetration into the wood (Laksono et al. 2023; Wahyuningtyas et al. 2022).

Nano-magnetite (Fe_3O_4-NP) was also selected as an impregnation material in this study, considering its high magnetic properties, easy processing, inexpensive cost, lack of toxicity, and many beneficial modification properties (Gao et al. 2015; Tukan et al. 2023). Researchers have investigated numerous nano-magnetite applications, namely as an absorbent of heavy metal removals, sensors, catalysts, pigments, ferrofluids, drug deliveries, and many more (Dong et al. 2012; El-Dib et al. 2020; Lou et al. 2008). The co-precipitation method can synthesize this chemical using a weak base precursor of ammonium hydroxide (NH_4OH). NH_4OH added during the synthesis process also results in particles of uniform size, which supports the effectiveness of its penetration into the wood (Jayaprakash et al. 2014).

Magnetic wood can be applied in many industries, including electronics, the military, healthcare instruments, interior home decorations, and eco-friendly building constructions (Liu et al. 2022; Oka et al. 2012; Trey et al. 2014). This invention is necessary because electromagnetic waves can cause many health problems. Magnetic wood, as an electromagnetic shielding material, considers the anisotropic morphology of nano-magnetite sediment in the wood cavities, which leads to the multilayer structure in magnetic wood (Cheng et al. 2020). These structures are advantageous because they will provide a great deal of magnetic loss tangent, achieve perfect impedance matching, and create an interconnected 3D network that allows electromagnetic wave absorption, reflection, and attenuation (Lou et al. 2018; Merk et al. 2014). So, this study is conducted to convert sengon wood into magnetic wood through the impregnation process using nano-magnetite synthesized by the co-precipitation method and commercial nano-magnetite. In addition, we also compared the superiority of both nano-magnetites in absorbing electromagnetic waves.

2. Materials and Methods

2.1. Materials

A six-year-old sengon wood (*F. moluccana*) was obtained from a community forest in Sukabumi, West Java (6° 57' 21.1" S and 106° 53' 29.3" E), with a diameter at breast height of 25–28 cm. The chemicals used were magnetite (Fe_3O_4) nanoparticles (diameter 297 nm ± 5 nm; Nanjing Aocheng Chemical Co., China), $FeCl_3 \cdot 6H_2O$ (Merck, United States), $FeCl_2 \cdot 4H_2O$ (Merck, United States), ammonium hydroxide (NH_4OH) 25% (Merck, United States), ethylenediaminetetraacetic acid (EDTA) (Merck, United States), and additional supplies included pH paper and deionized water.

2.2. Methods

2.2.1. Wood sample preparation

Sengon wood was cut into several dimensions without distinguishing sapwood and heartwood portions by the different standards of each test. The number of samples required was five repetitions for each treatment. For further information, the sample dimensions can be seen in **Table 1**.

Table 1. The sample dimensions for each test

No.	Tests	Dimensions	References
1	Color spectra measurement	2 × 5 × 6 cm^3	Christie (2015)
2	Physical properties (weight percent gain, density)	2 × 2 × 2 cm^3	BSI (1957)
3	Hardness	5 × 5 × 15 cm^3	ASTM (1994)
4	Vector Network Analyzer (VNA)	2 × 2 × 2 cm^3	-

2.2.2. Synthesis of nano-magnetite

This method was developed following the work of Daoush (2017). The synthesis of nano-magnetite used weak base precursor NH_4OH and a mixture of Fe^{3+} and Fe^{2+} (molar ratio of 2:1) in 200 mL of deionized water. Then, 0.292 g of EDTA dissolved in 100 mL of deionized water was

added to the solution and stirred using a magnetic stirrer for 15 minutes. The solution was vacuumed at 1 bar for 15 minutes, and NH_4OH was added gradually until it reached pH 12 and formed magnetite nanoparticles indicated by black sediment at the base of the glass beaker. Subsequently, the synthesized nano-magnetite was neutralized by washing the solution with deionized water. The washing continued until the pH reached 9, then nano-magnetite particles were separated and placed in an oven at 45°C. A fine black powder produced from this process was then measured using a Particle Size Analyzer (PSA) (LS 13 320 XR, Beckman Coulter, United States).

2.2.3. Preparation of impregnation solution

The nano-magnetite solution was determined in w/v (g/mL) for optimal results. Nano-magnetite solutions were prepared at three concentration levels: 1%, 2.5%, and 5%. These solutions were mixed for 10 minutes using a probe-type sonicator (CGOLDENWALL 300W Ultrasonic Homogenizer Sonicator 5-200MLLab, manufactured in China) at an amplitude of 40%. Nano-magnetites have characteristics that are insoluble in water; however, the nano-magnetites that resulted in this study were nanometer-sized. Furthermore, using a sonicator in this stage aimed to increase the solubility of nano-magnetite in water (Schwertmann et al. 2003; Sompech et al. 2012).

2.2.4. Magnetic wood impregnation

Laksono et al. (2023) adopted the impregnation process in this study. This process was carried out by the ex-situ method using synthetic nano-magnetite compared to commercial nano-magnetite as the impregnation solution. The magnetic wood manufacturing process can be seen in the following **Fig. 1**.

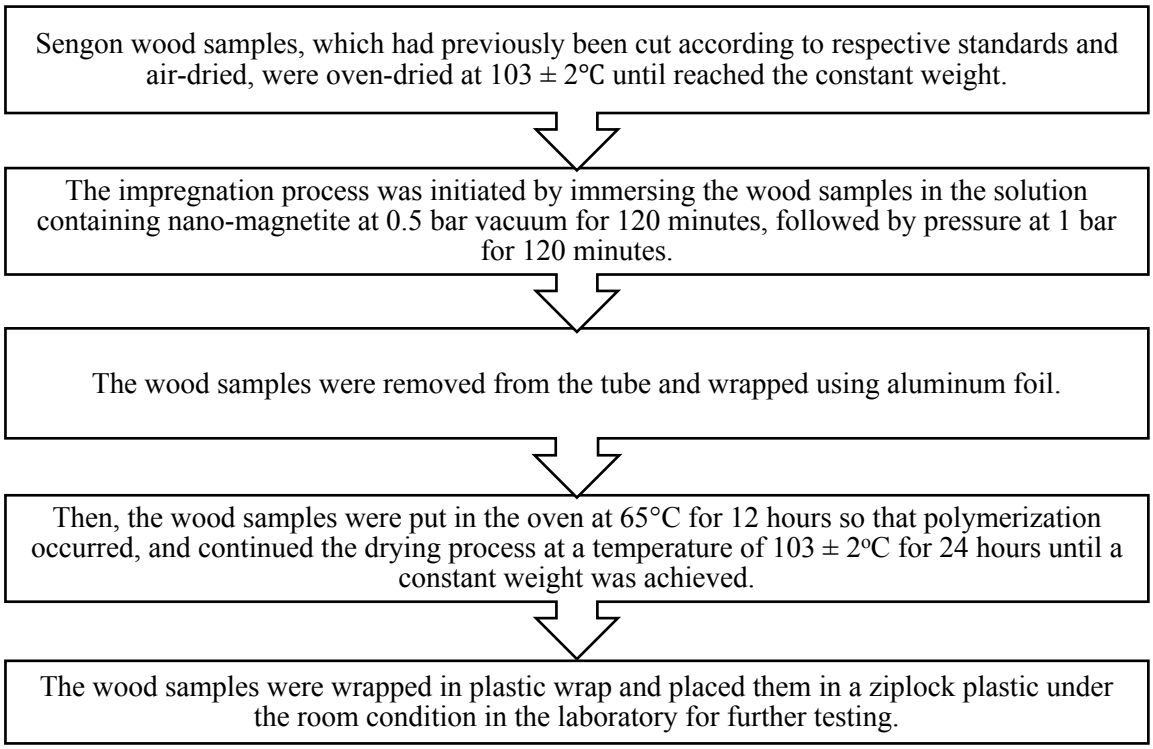

Fig. 1. The procedure of the impregnation process.

2.3. Physical and Mechanical Properties Measurement

2.3.1. Physical properties of magnetic wood

The physical properties tested on sengon wood were weight percent gain (WPG) and density. WPG is the percentage ratio of the weight of impregnated wood to its initial weight (Rahayu et al. 2020). Hill (2006) stated that the WPG of modified wood can be calculated using Equation 1.

$$WPG\ (\%) = \frac{W_1 - W_0}{W_0} \times 100\% \quad (1)$$

where W_0 is the oven-dried weight of samples before the impregnation (g), and W_1 is the oven-dried weight of samples after the impregnation (g). On the other hand, the density of sengon wood after the impregnation process was determined using Equation 2.

$$\rho\ (kg/m^3) = \frac{W_1}{V_1} \quad (2)$$

where W_1 is the oven-dried weight samples after impregnation (g), and V_1 is the oven-dried volume samples after impregnation (cm^3).

2.3.2. Wood color change evaluation

The most common method to measure wood discoloration is CIE L*, a*, and b* color space with a three-axis system. The wood samples were scanned using CanoScan Lide 300 (Canon Singapore Pte. Ltd.). Each sample was measured three times in three predetermined points to find the L, a, and b values. Wood color was measured using Adobe Photoshop CS 4 software (Muflihati et al. 2014). The L* value expresses the brightness parameter on a scale of zero (black) – 100 (white). The a* value represents the red-to-green color parameters. The +a* value (0 to +80) is for red, and the –a value (0 to -80) is for green. Meanwhile, the b value states the parameters for blue to yellow. The value is +b (0 to +70) for yellow and –b (0 to -70) for blue (Christie 2015). An illustration of the wood sample is shown in **Fig. 2**.

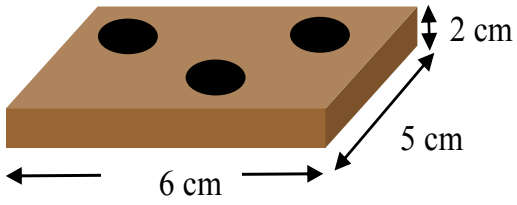

Fig. 2. The wood sample illustration for color change measurement.

The discoloration of modified wood (ΔE) can be defined using Equation 3.

$$\Delta E = \sqrt{(\Delta L)^2 + (\Delta a)^2\ (\Delta b)^2} \quad (3)$$

where ΔE is a parameter to determine the changes in wood color brightness visibly, ΔL is the brightness differences of sengon wood before and after treatments, Δa is the red or green color differences of sengon wood before and after treatments, where Δb is the yellow or blue color differences of sengon wood before and after treatments.

The overall discoloration of sengon wood was evaluated based on the distribution rules of discoloration according to Barcík et al. (2015), presented in **Table 2**.

Table 2. The overall color change (ΔE^*) evaluation criteria

Color differences	Effects
$0.2 < \Delta E^*$	Invisible difference
$0.2 \leq \Delta E^* < 2$	Small difference
$2 \leq \Delta E^* < 3$	Color change visible with a high-quality filter
$3 \leq \Delta E^* < 6$	Color change visible with medium-quality filter
$6 \leq \Delta E^* < 12$	High color changes
$\Delta E^* \geq 12$	Different color

2.3.3. Hardness test

The hardness test was conducted according to the Janka by inserting a 1.128 ± 0.005 cm diameter hemispherical steel ball on the wood. This test was aimed to determine the required load until the ball had penetrated to half its diameter (0.564 cm) upon the sample surface. Equation 4 was used to determine the hardness (H) of treated wood.

$$H\ (kg/cm^2) = \frac{P_{max}}{A} \quad (4)$$

where P_{max} is the maximum load (kg) applied to the wood sample, and A is the cross-sectional area to which the load is applied.

2.4. Electromagnetic Waves Absorbance Measurement

The microwave absorption properties of magnetic wood were characterized using Vector Network Analyzer (R3370, Advatest, Japan). This instrument has a frequency range of 8 to 20 GHz. The reflection loss (RL) curve is obtained by scattering parameters measurement in the form of the S_{11} model (reflection coefficient) from the source of electromagnetic waves.

2.5. Data Analysis

Statistical analysis using a completely randomized factorial design by IBM SPSS 25 was performed to evaluate two factors applied: the type of nano-magnetite (synthetic and commercial) and the solution concentration (untreated, 1%, 2.5%, and 5%). These factors were analyzed using ANOVA followed by the Duncan test on $\alpha = 5\%$.

3. Results and Discussion

3.1. Size Distribution of Synthetic and Commercial Nano-Magnetite

This study used two types of nano-magnetite (Fe_3O_4-NP), namely commercial and synthesized. The nano-magnetite synthesis process used the co-precipitation method with weak base precursors: ammonium hydroxide (NH_4OH) and ethylenediaminetetraacetic acid (EDTA). The co-precipitation method was selected based on its high level of ease on a laboratory scale and generated a high yield value (Dubey and Kain 2018), reaching 92.71%. In addition, this co-precipitation method is also used as a comparison that correlates with its application for the manufacture of magnetic wood, which previously used the in-situ method through the formation of nano-magnetite directly in the wood pore (Rahayu et al. 2022). In the nano-magnetite synthesis process, the use of NH_4OH as a base precursor and EDTA as a capping agent was chosen because it can control the growth of magnetite nuclei to produce smaller magnetite particle sizes and have

a more uniform morphology (Jayaprakash et al. 2014). The addition of EDTA can also support nucleation to reduce particle size (Magdalena et al. 2018), increase stabilization, reduce the activation energy of nanoparticles (Fumis et al. 2022), and increase adsorption capacity by increasing the surface area of nano-magnetite (Wang et al. 2012). This can be proven by referring to the results of the nano-magnetite analysis with PSA, which appears below (**Fig. 3**).

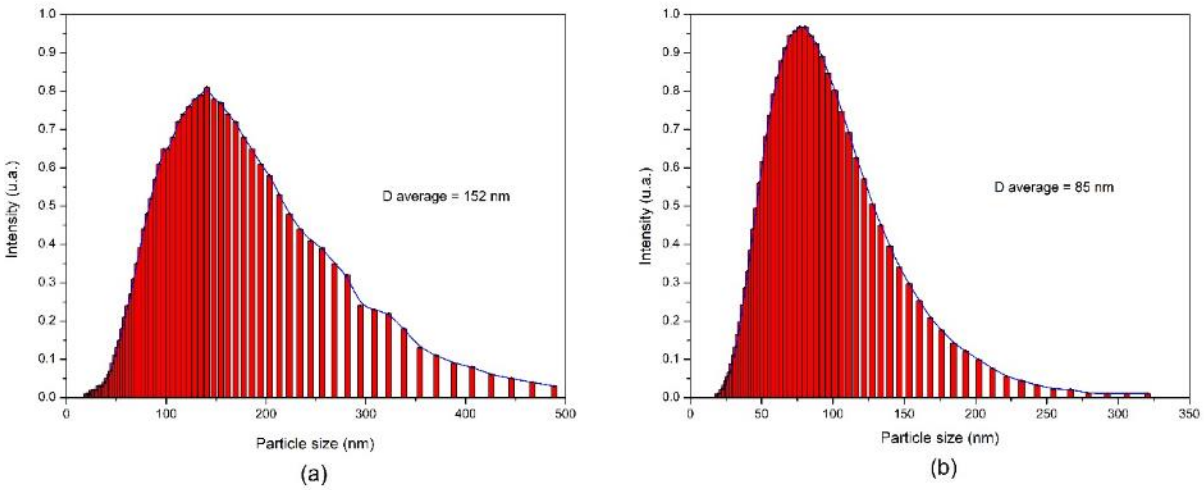

Fig. 3. Size distribution of (a) commercial nano-magnetite and (b) synthetic nano-magnetite produced by the co-precipitation method with a weak base precursor.

Based on the results of nano-magnetite particle size analysis using PSA, it can be seen that the particle size distribution range for commercial nano-magnetite is 20–489 nm with the highest intensity at 141 nm and an average particle size of 152 nm while the synthesized nano-magnetite is 19–320 nm with the highest intensity at 80 nm and an average particle size of 85 nm. This shows that the synthesized nano-magnetite has better quality than the commercial one because it has a length of less than 100 nm so that it can be categorized as nanoparticles (Khan et al. 2019) and has a more uniform particle distribution to be applied to sengon wood in the manufacture of magnetic wood by the ex-situ method. EDTA was thought to successfully coat the nano-magnetite surface and reduce its surface energy, thereby reducing the possibility of accumulation. This enhanced the solubility and stability of nano-magnetite through sonication and also improved its dispersibility, thus allowing better penetration into the wood (Fumis et al. 2022; Magdalena et al. 2018; Wang et al. 2012). Nevertheless, there is still a possibility that agglomeration and oxidation will continue to occur, especially in commercial nano-magnetite, because nano-magnetite has strong dipole attraction among its particles (Masoudi et al. 2012; Theerdhala et al. 2010).

3.2. Physical Properties of Magnetic Wood

The physical properties test in this study included the WPG and the density of impregnated sengon wood with two different types of nano-magnetite. The higher WPG of the wood indicated the amount of chemicals that penetrated the wood after impregnation. The highest WPG of impregnated wood was obtained by the concentration of 5% for each treatment. It appeared in **Table 3** that there was a significant increase in the WPG of impregnated sengon wood after impregnation treatment, along with the addition of nano-magnetite concentration. Like Fadia et al. (2023b), nano-magnetite concentration and WPG also had a positive correlation. The nano-

magnetite was suspected to fill the wood cavities, increasing wood weight (Marques et al. 2006). However, the WPG value of commercial nano-magnetite is higher than synthetic nano-magnetite despite no significant difference between the WPG of both synthetic and commercially produced nano-magnetite. Both impregnation solutions used demineralized water to dissolve the nano-magnetite particles. According to Prihatini et al. (2022), the solution containing nano-magnetite and demineralized water separated into solid and liquid phases or did not form a colloidal phase. Therefore, the WPG of sengon wood is relatively low even though there is a slight increase after the concentration increases.

Table 3. The physical properties of sengon wood after impregnation treatment

Wood Samples	WPG (%)	Density (g/cm^3)
Untreated wood	0.42 ± 0.22^{a}	0.27 ± 0.06^{a}
SNM 1%	1.34 ± 0.33^{b}	0.28 ± 0.03^{ab}
SNM 2.5%	3.62 ± 0.16^{c}	0.30 ± 0.03^{ab}
SNM 5%	5.82 ± 0.99^{d}	0.30 ± 0.02^{bc}
CNM 1%	1.32 ± 0.16^{b}	0.28 ± 0.02^{bc}
CNM 2.5%	3.76 ± 0.44^{c}	0.31 ± 0.03^{c}
CNM 5%	6.00 ± 0.35^{d}	0.31 ± 0.04^{c}

Notes: ^{a,ab,b,bc,c,d} are Duncan's test results ($P < 0.05$), SNM is synthetic nano-magnetite, CNM is commercial nano-magnetite, and WPG is weight percent gain.

In line with WPG, the density of impregnated sengon wood with nano-magnetite is also increased compared to wood without chemical treatment (untreated). The highest density of both is achieved at a concentration of 5%. **Table 3** shows that the statistical analysis of the types of nano-magnetite was insignificantly different in density, in contrast to the concentration of nano-magnetite, which slightly affects the density. Bowyer et al. (2007) concluded that the wood cell wall becomes denser due to the chemical entering the wood when the concentration level increases further. This makes sengon wood more dimensionally stable when temperature and humidity change. Accordingly, this condition means the wood does not readily absorb water and is protected from biological attacks, such as mold, fungi, bacteria, and insects (Garskaite et al. 2021).

3.3. Wood Discoloration

The color change of sengon wood after impregnation with synthetically and commercially produced nano-magnetite is illustrated in **Fig. 4**. As previously predicted, impregnated sengon wood tends to have lower L*, a*, and b* values than untreated wood, which showed the highest brightness value before and after impregnation treatment. This is very different from the SNM and CNM wood. A study by Muflihati et al. (2014) revealed that the rising L* value of wood indicates an intensification of its brightness, while lowering L* values suggest wood discoloration. By continuing to add nano-magnetite concentration in this research, the color of the impregnated sengon wood became darker. There was also a lowering brightness of magnetic wood (L* value) after the impregnation process, as shown in **Fig. 4**. The SNM 1% exhibited a significant reduction in brightness, followed by SNM 2.5% and SNM 5%, which continued to decrease in brightness level. The red value (a#) of SNM 1% slightly increased but did not cause a significant difference; meanwhile, SNM 2.5% and SNM 5% show constant values. This is somewhat different from the yellow value (b#) in that there was a slightly decreasing value in SNM 1%, then SNM 2.5% and SNM 5% keep showing a little subtraction trend.

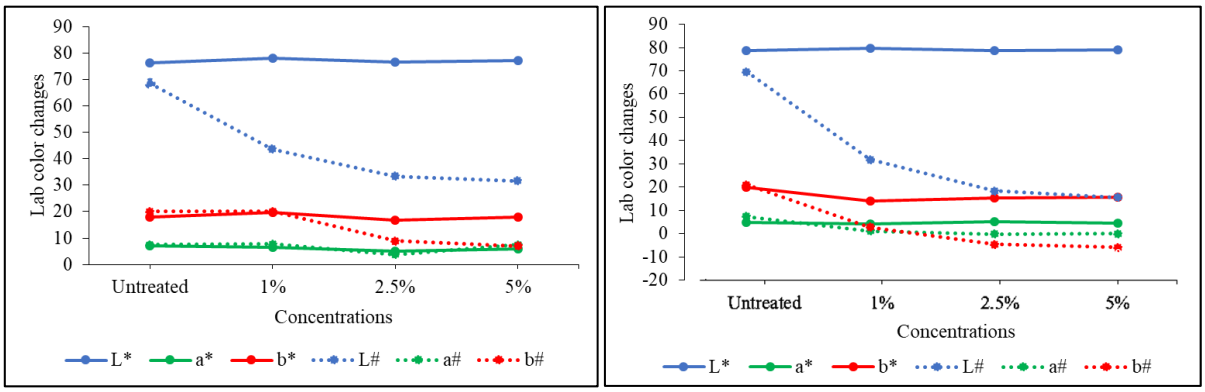

Fig. 4. The L*, a*, and b* values before treatment and the L#, a#, and b# values after treatment of (a) the SNM wood and (b) the CNM wood.

Along with synthetic nano-magnetite, commercial nano-magnetite also provided a darkening color effect to sengon wood samples. It can be analyzed from **Figs. 4a and 4b** indicate a sharp decline in sengon wood brightness after being incorporated with commercial nano-magnetite, indicated by the L# value. In addition, there was also a slight reduction in the red value (a#), although this parameter does not show visible changes in the SNM wood. On the other hand, the decrease in yellow value (b#) occurred dramatically more than expected. This phenomenon also happened in the magnetic wood manufactured by Rahayu et al. (2022). That magnetic wood color turned black due to using NH_4OH as a weak base precursor, resulting in nano-magnetites with small particle sizes distributed uniformly. However, Merk et al. (2014) also assumed that the brownish-black color of magnetic wood indicates contamination with rust or corrosion. The visual appearance of the SNM and CNM magnetic wood is shown in the following **Fig. 5**.

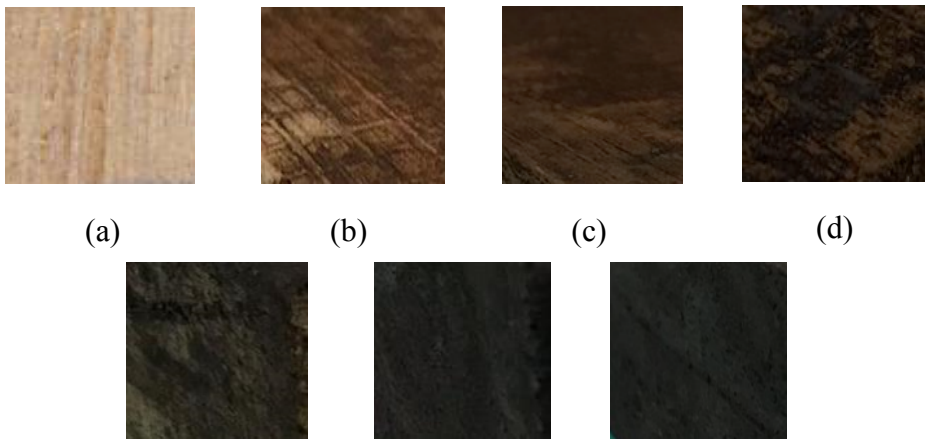

Fig. 5. Sengon wood color after being impregnated (a) untreated, (b) SNM 1%, (c) SNM 2.5%, (d) SNM 5%, (e) CNM 1%, (f) CNM 2.5%, and (g) CNM 5%.

The color of the impregnated wood is known to have darkened immediately after the impregnation process was done. It can be seen that untreated wood is light brown (**Fig. 5a**), then turned into dark brown at a concentration of 1% of the SNM wood (**Fig. 5b**). Then, the SNM wood color got darker with the addition of nano-magnetite concentration into 2.5% and 5%, as shown in **Figs. 5c** and **5d**. This incident was also experienced by Gao et al. (2023), who also changed the

color of the balsa wood from red/orange to dark green/black as exposed nano-magnetites. This was caused by the interaction between nano-magnetite and lignin components within the wood. An electrostatic attraction, Van Der Waals force, and hydrogen bond played roles in binding the nano-magnetite with lignin. Hence, the bonds are formed among them, resulting in wood discoloration (Zheng et al. 2021). The presence of nano-magnetite on the sengon wood surface also contributed to the large specific surface area of wood samples, corresponding to the large specific surface area of nano-magnetite particles (Feng et al. 2023).

In addition, even if nano-magnetite concentration was added, it could still maintain the wood structure. Similar to the SNM wood, the darkening of the CNM wood color is genuinely different from untreated wood after interacting with commercial nano-magnetite. The color gradient gets darker with the addition of nano-magnetite concentration, even though they were darker than the SNM wood, as displayed in **Fig. 5e-g**. Wahyuningtyas et al. (2022) also synthesized magnetic wood using commercial nano-magnetite and produced a black color. This is associated with the WPG and density of magnetic wood, which also increased because plenty of nano-magnetite is deposited in the wood cell walls. The color of CNM 5% (**Fig. 5g**) became darkest among other samples since the cell cavities were being saturated with nano-magnetite in the tangential section and indicated even adhesion of nano-magnetite to the sengon wood (Garskaite et al. 2021).

The analysis results mentioned remarkable differences in the sengon wood color after impregnation treatment that were affected by synthetic and commercial nano-magnetite, as presented in **Fig. 6**.

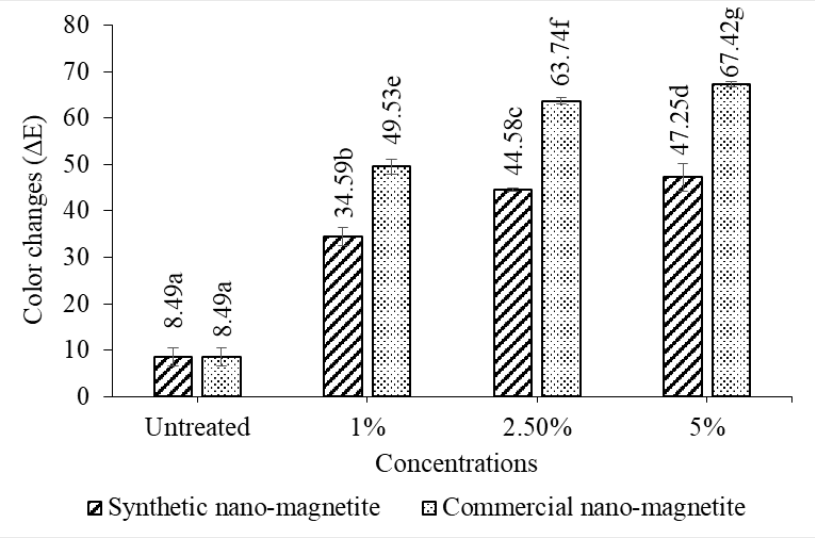

Fig. 6. The discoloration of sengon wood after being impregnated with synthetic and commercial nano-magnetite.

The highest discoloration values of both types of nano-magnetite were achieved at the concentration of 5%. However, the CNM wood's discoloration was more significant than the SNM wood. The additional nano-magnetite concentration also positively impacts the darkening of wood color. This transformation occurred because the co-precipitation method resulted in a smaller size of nano-magnetite, so the wood underwent an inorganic mineralization process in which nano-magnetite particles were deposited in the interconnected porous network structured wood substrate (Cheng et al. 2020). Based on the overall color change evaluation criteria, all the SNM and CNM

have ΔE values of more than 12, meaning the wood color has changed significantly from its original color or become a different color.

3.4. Wood Hardness

In addition to testing the physical properties and color of wood, the mechanical properties of modified wood also need to be tested. The user considers the mechanical properties, such as strength, hardness, and wear resistance of wood to be crucial factors in determining its quality, and these parameters are also necessary. In this study, only hardness was evaluated because wood hardness acts as a parameter to measure the manufactured wood materials' resistance and predict its performance. This is also used to assess the effectiveness of the modification process. The hardness test was carried out according to the Janka test method after air-conditioning samples at 20°C and relative humidity (RH) of approximately 65%, which achieved an equilibrium moisture content of untreated wood. **Fig. 7** below shows the hardness of sengon wood after the impregnation process.

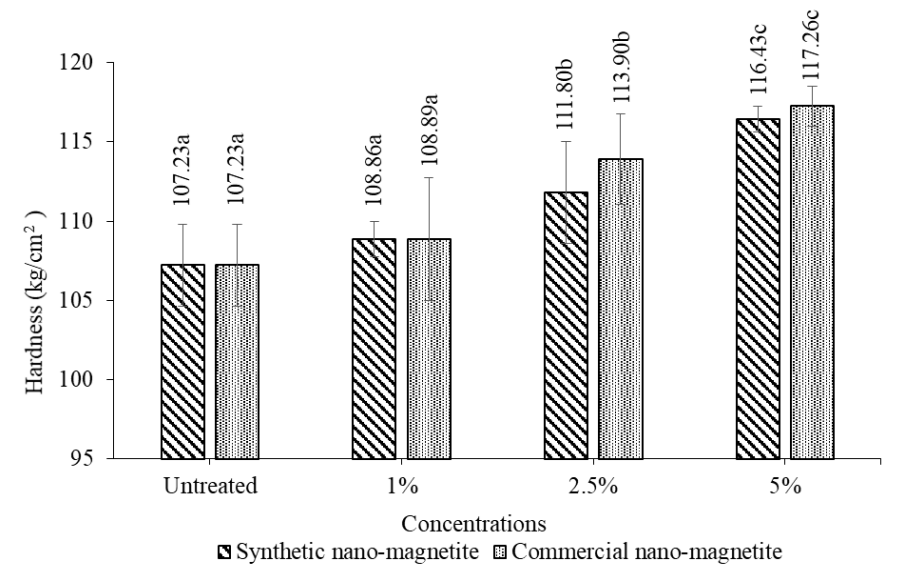

Fig. 7. The increasing sengon wood hardness after impregnation treatment.

Based on **Fig. 7**, the highest hardness is obtained at a concentration of 5% for SNM and CNM wood samples. Interaction between the types of nano-magnetite and the concentration did not point out a noticeable effect on hardness, while the nano-magnetite addition levels caused a significant upward trend. Cell wall deformation occurred due to the reduced wood porosity, so the wood cavity was filled with chemicals, causing the intercellular space of the wood also to decrease (Mania et al. 2020). This is affected by the increasing WPG and density of sengon wood after incorporating it with nano-magnetite, so the sengon wood hardness also increased (Rahayu et al. 2021). In addition, it is known that the hardness of wood depends on some wood conditions during testing, such as the force applied to the wood, the cross-section of wood being tested, the weight percentage of reinforcement materials, sintering temperatures, wood density, fiber size, and intercellular bonds among the wood fiber (Heräjärvi et al. 2004; Ashrafi et al. 2022). A good crystallite structure guarantees the materials' high mechanical and magnetic properties. As stated by Teng et al. (2018) and Prihatini et al. (2023), the vacuum-pressure impregnation technique supports the chemicals to get into the wood more quickly and bond to the cell wall components

than other techniques. The different mechanical properties of wood are also influenced by nano-magnetite impregnation treatment, as demonstrated by Geeri et al. (2023).

3.5. Electromagnetic Waves Absorption Properties

Electromagnetic wave shielding materials are needed to protect humans and the environment. Electromagnetic waves are commonly produced by currents in wires and circuits from electronic devices. VNA aims to characterize the absorption properties of materials against electromagnetic waves. To determine the RL and absorption behavior released by magnetic wood, this instrument must use an 8–12 GHz frequency range. The working mechanism of this instrument ensures that waves are reflected when they hit metallic materials, transmitted when they hit transparent materials, and absorbed when applied to absorber materials (Lumen and OpenStax 2021). In this test, untreated wood shows zero RL, frequency, and absorption because there was no chemical treatment on the wood (**Fig. 8**). Conversely, the SNM and CNM wood indicate increased magnetic parameter values. Aini et al. (2016) stated that a high RL value indicates a higher material absorption capacity for electromagnetic waves. On the other hand, the absorption coefficient value shows the ability to absorb microwaves, as Wardiyati et al. (2018) explain.

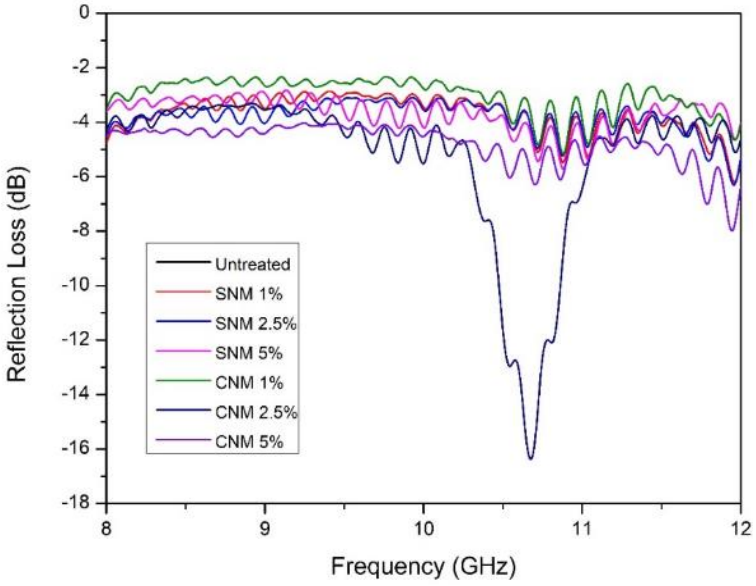

Fig. 8. The electromagnetic wave absorption by magnetic sengon wood in various treatments.

It can be concluded from **Fig. 8** that the SNM wood samples obtained the highest RL and absorption, respectively, at the concentration of 2.5%, namely -20.58 dB and 99.13%, at the frequency of 11.20 GHz. The lower RL, frequency, and absorption in SNM 1% were due to the lack of dielectric material. Hence, combining or adding more dielectric material to this wood sample is necessary to improve its absorption range, specifically by increasing the nano-magnetite concentration, according to Silvia et al. (2021). These results also prove that synthetic nano-magnetite has a higher wave absorption rate than commercial nano-magnetite. Following the statement of Kong et al. (2010), synthetic nano-magnetite is a good electromagnetic absorber in a polymer matrix composite. For further information, the RL, frequency, and absorption values of magnetic sengon wood are listed in **Table 4**.

Table 4. The VNA test results of magnetic sengon wood

Treatments	*Reflection Loss* (dB)	Frequency (GHz)	Absorption (%)
Untreated	0.00	0.00	0.00
SNM 1%	-9.26	8.38	88.14
SNM 2.5%	-20.58	11.20	99.13
SNM 5%	-18.49	11.36	98.59
CNM 1%	-13.76	11.36	95.79
CNM 2.5%	-13.32	11.54	95.34
CNM 5%	-15.03	11.20	97.35

Notes: SNM is synthetic nano-magnetite, and CNM is commercial nano-magnetite.

Synthetic and commercial nano-magnetite can absorb more than 90% of electromagnetic waves emitted by electronic devices. Synthetic nano-magnetites are primarily known to have higher absorption than commercial nano-magnetites. This finding is thought to be due to the use of a weak base precursor NH_4OH, which homogenized the size of the resulting nano-magnetite and accelerated the crystallite formation of nano-magnetite (Peternele et al. 2014). Bostanabad et al. (2015) also observed that the lower absorption could be caused by the crack initiation and failure of the coating layer, in this case EDTA, followed by the reduction of the ferri-magnetic phase of nano-magnetite. The thin coating layer makes the nano-magnetite easily agglomerate and clog the wood pores, so only a small amount penetrates the wood.

Magnetic properties of magnetic wood are also affected by the immersion time in the solution due to the electric polarization and conductivity. Moreover, materials may also exhibit strong fluctuations due to their chemical composition. For example, oxygen in wood and nano-magnetite causes electric dipole polarization. The polarization is determined by the difference in the available valence and the amount of electron transfer between Fe^{3+} and Fe^{2+} ion positions (Geeri et al. 2023; Xu et al. 2013). An increase in RL and frequency also correlates with the wood microstructure, wood-water interaction, dielectric behavior, material thickness, material concentration, permeability, and complex permittivity depending on the shapes, properties, and size. It has been observed that the enhancing value of RL decreases the wood's relative permittivity with increasing frequency of wood and fiber orientation (Silvia et al. 2021; Zakaria et al. 2021). Therefore, based on the above results, SNM wood can absorb more electromagnetic waves than CNM wood because it can absorb almost 100% of electromagnetic waves with only a concentration of 2.5%.

Many studies have investigated the utilization of magnetic wood. The combination of wood and nano-magnetite particles is brilliant for sensors, active fillers, core materials of power inductors and transformers, medical devices, and electromagnetic wave absorbers. Moreover, using wood can reduce the possibility of corrosion, oxidation, noise, and even burns due to being exposed to the heat of electronic devices operation for a long time (Martins et al. 2023). With these obtained absorbance levels, both kinds of magnetic wood produced from this study can be applied as electromagnetic wave shielding materials. Several electronic devices are known to emit electromagnetic waves in various frequency bands, such as wireless local area networks (2–6 GHz), Bluetooth (2.4 GHz), mobile phones (0.3–3 GHz), and military radar (8–12 GHz) (Chikyu et al. 2020). So, installing magnetic wood as an electromagnetic wave absorber in the house interior is very appropriate to prevent various health problems.

4. Conclusions

Magnetic wood was fabricated by the impregnation process using two different types of nano-magnetite, namely nano-magnetite obtained from the co-precipitation method and commercial nano-magnetite. The CNM wood showed more improvements in WPG, density, and hardness than the SNM wood, even though both types of nano-magnetite did not provide different effects in these parameters. There was also a significant reduction in brightness value after interacting with nano-magnetite as the concentration increased. The overall discoloration was more pronounced in the CNM wood than in the SNM wood because the CNM wood produced a darker color. The absorption capacity of the SNM wood was more significant than that of the CNM wood, as it can absorb almost 100% of the material with only 2.5% nano-magnetite concentration. This modification treatment can answer the question of expanding the sengon wood utilization by converting sengon wood into an electromagnetic wave shielding material. With various considerations from the results, producing this instrument with the optimal treatment, namely, SNM 5%, is adequate.

References

Aini, N., Widyastuti, W., and Fajarin, R. 2016. Pengaruh Jenis Polimer terhadap Reflection Loss pada *Polymer Matrix Composite* (PMC) Barium Heksaferrit sebagai Radar Absorbing Material (RAM). *Jurnal Teknik ITS* 5(2): 125–129. DOI: 10.12962/j23373539.v5i2.17710

Ashrafi, N., Ariff, A. H. M, Jung, D. W., Sarraf, M., Foroughi, J., Sulaiman, S., and Hong, T. S. 2022. Magnetic, Electrical, and Physical Properties Evolution in Fe_3O_4 Nanofiller Reinforced Aluminium Matrix Composite Produced by Powder Metallurgy Method. *Materials* 15(12): 4153. DOI: 10.3390/ma15124153

ASTM. 1994. ASTM D143-94: Standard Test Methods for Small Clear Specimens of Timber. American Society for Testing and Materials (ASTM), Pennsylvania, United States. DOI: 10.1520/d0143-23

Barcík, S., Gašparík, M., and Razumov, E. 2015. Effect of Thermal Modification on the Wood Colour Changes of Oak Wood. *Research for Rural Development* 2(3): 87–92. DOI: 10.1007/s10086-018-1721-0

Bostanabad, K., Kianvash, A., and Entezami, A. 2015. Investigation on Magnetic and Microwave Behavior of Nanomagnetite Coated Carbon Fibers Composite. *Journal of Particle Science and Technology* 1(2): 85–90. DOI: 10.22104/jpst.2015.85

Bowyer, J. L., Shmulsky, R., and Haygreen, J. G. 2007. *Forest Products and Wood Science - An Introduction. Iowa State University Press: Vol. Mc (5th Editio, Issue 3)*. Blackwell Publisher, New Jersey. DOI: 10.1002/9780470960035

BSI. 1957. BS-373: Standard Methods of Testing Small Clear Specimens of Timber. British Standards Institution (Daoush), London, United Kingdom.

Cheng, Z., Wei, Y., Liu, C., Chen, Y., Ma, Y., Chen, H., Liang, X., Sun, N. X., and Zhu, H. 2020. Lightweight and Construable Magnetic Wood for Electromagnetic Interference Shielding. *Advanced Engineering Materials* 22: 2000257. DOI: 10.1002/adem.202000257

Chikyu, N., Nakano, T., Kletetschka, G., and Inoue, Y. 2020. Excellent Electromagnetic Interference Shielding Characteristics of a Unidirectionally Oriented Thin Multiwalled Carbon Nanotube/Polyethylene Film. *Materials and Design* 195: 108918. DOI:

10.1016/j.matdes.2020.108918

Christie, R. 2015. *Colour Chemistry: 2nd edition*. Royal Society Chemistry, London. DOI: 10.1039/bk9781849733281-00072

Darmawan, W., Nandika, D., Massijaya, Y., Kabe, A., Rahayu, I., Denaud, L., and Ozarska, B. 2015. Lathe Check Characteristics of Fast Growing Sengon Veneers and Their Effect on LVL Glue-Bond and Bending Strength. *Journal of Materials Processing Technology* 215(2): 181–188. DOI: 10.1016/j.jmatprotec.2014.08.015

Daoush, W. M. 2017. Co-Precipitation and Magnetic Properties of Magnetite Nanoparticles for Potential Biomedical Applications. *Journal of Nanomedicine Research* 5(3): 12–16. DOI: 10.15406/jnmr.2017.05.00118

Dong, F., Guo, W., and Ha, C. S. 2012. Monodisperse Single-Crystal Mesoporous Magnetite Nanoparticles Induced by Nanoscale Gas Bubbles. *Journal of Nanoparticle Research* 14: 1303. DOI: 10.1007/s11051-012-1303-9

Dong, Y., Yan, Y., Zhang, Y., Zhang, S., and Li, J. 2016. Combined Treatment for Conversion of Fast-Growing Poplar Wood to Magnetic Wood with High Dimensional Stability. *Wood Science and Technology* 50(3): 503–517. DOI: 10.1007/s00226-015-0789-6

Dubey, V., and Kain, V. 2018. Synthesis of Magnetite by Coprecipitation and Sintering and its Characterization. *Materials and Manufacturing Processes* 33(8): 835–839. DOI: 10.1080/10426914.2017.1401720

El-Dib, F. I., Mohamed, D. E., El-Shamy, O. A. A., and Mishrif, M. R. 2020. Study the Adsorption Properties of Magnetite Nanoparticles in the Presence of Different Synthesized Surfactants for Heavy Metal Ions Removal. *Egyptian Journal of Petroleum* 29(1): 1–7. DOI: 10.1016/j.ejpe.2019.08.004

Fadia, S. L., Rahayu, I., Nawawi, D. S., Ismail, R., and Prihatini, E. 2023a. Magnetic Characteristics of Sengon Wood-Impregnated Magnetite Nanoparticles Synthesized by the Co-Precipitation Method. *AIMS Materials Science* 11: 1–27. DOI: 10.3934/matersci.2024001

Fadia, S. L., Rahayu, I., Nawawi, D. S., Ismail, R., and Prihatini, E. 2023b. The Physical and Magnetic Properties of Sengon (*Falcataria moluccana*) Wood Impregnated with Synthesized Magnetite Nanoparticles. *Jurnal Sylva Lestari* 11(3): 408–426. DOI: 10.23960/jsl.v11i3.761

Feng, W., Xu, Q., Zhao, J., Zhang, W., Yu, Y., Qian, G., Fu, L., Chen, C., and Min, D. 2023. Wood-Based Magnetic/Conductive Composite Material with High Dielectric Constant and Absorption Dominance for High-Efficiency EMI Shielding. *Social Science Research Network* 1–38. DOI: 10.2139/ssrn.4665330

Fumis, D. B., Silveira, M. L. D. C., Gaglieri, C., Ferreira, L. T., Marques, R. F. C., and Magdalena, A. G. 2022. The Effect of EDTA Functionalization on Fe_3O_4 Thermal Behavior. *Materials Research* 25. DOI: 10.1590/1980-5373-mr-2022-0312

Gao, J., Guo, Z., Yu, S., Su, F., Ma, H., Du, B., Wei, Q., and Pang, X. 2015. A Novel Controlled Release System-Based Homogeneous Immunoassay Protocol for SCCA Using Magnetic Mesoporous Fe_3O_4 as a Nanocontainer and Aminated Polystyrene Microspheres as a Molecular Gate. *Biosensors and Bioelectronics* 66: 141–145. DOI: 10.1016/j.bios.2014.10.078

Gao, Y., Yang, X., Garemark, J., Olsson, R. T., Dai, H., Ram, F., and Li, Y. 2023. Gradience Free Nanoinsertion of Fe_3O_4 into Wood for Enhanced Hydrovoltaic Energy Harvesting. *ACS*

Sustainable Chemistry and Engineering 11(30): 11099–11109. DOI: 10.1021/acssuschemeng.3c01649

Garskaite, E., Stoll, S. L., Forsberg, F., Lycksam, H., Stankeviciute, Z., Kareiva, A., Quintana, A., Jensen, C. J., Liu, K., and Sandberg, D. 2021. The Accessibility of the Cell Wall in Scots Pine (*Pinus sylvestris* L.) Sapwood to Colloidal Fe_3O_4 Nanoparticles. *ACS Omega* 6(33): 21719–21729. DOI: 10.1021/acsomega.1c03204

Geeri, S., Murthy, B. K., Kolakoti, A., Murugan, M., Elumalai, P. V, Dhineshbabu, N. R., and Prabhakar, S. 2023. Influence of Magnetic Wood on Mechanical and Electromagnetic Wave-Absorbing Properties of Polymer Composites. *International Journal of Polymer Science* 2023: 1–12. DOI: 10.1155/2023/1142654

Hadi, Y. S., Herliyana, E. N., Mulyosari, D., Abdillah, I. B., Pari, R., and Hiziroglu, S. 2020. Termite Resistance of Furfuryl Alcohol and Imidacloprid Treated Fast-Growing Tropical Wood Species as Function of Field Test. *Applied Sciences* 10(17). DOI: 10.3390/app10176101

Hadiyane A., Dungani, R., Dewi, A. P., and Rumidatul, A. 2018. Effect of Chemical Modification of Jabon Wood (*Anthocephalus cadamba* Miq.) on Morphological Structure and Dimensional Stability. *Journal of Biological Sciences* 18: 201–207. DOI: 10.3923/jbs.2018.201.207

Hartono, R., Hidayat, W., Wahyudi, I., Febrianto, F., Dwianto, W., Jang, J. H., and Kim, N. H. 2016. Effect of Phenol Formaldehyde Impregnation on the Physical and Mechanical Properties of Soft-Inner Part of Oil Palm Trunk. *Journal of the Korean Wood Science and Technology* 44(6): 842-851. DOI: 10.5658/wood.2016.44.6.842

Heräjärvi, H. 2004. Variation of Basic Density and Brinell Hardness Within Mature Finnish *Betula pendula* and *B. pubescens* Stems. *Wood Fiber Science* 32(2): 216–227.

Hidayat, W., Suri, I. F., Febryano, I. G., Afkar, H., Rahmawati, L., Duryat, D., Kim, N. H. 2024. Elevating Timber Sustainability: Exploring Non-Chemical Wood Modification via Air Heat Treatment for Diverse Applications. *International Journal of Design and Nature and Ecodynamics* 19(1): 119-128. DOI: 10.18280/ijdne.190114

Hill, C. A. S. 2006. *Wood Modification: Chemical, Therma, and Other Processes*. John Willey and Sons Ltd., New Jersey. DOI: 10.1002/0470021748

Istikorini, Y., Faqih, A., Haneda, N. F., Siregar, U. J., and Andrianto, D. 2022. Effect of Endophytic Fungi on the Growth of Sengon (*Falcataria moluccana*). *Jurnal Sylva Lestari* 10(3): 321-332. DOI: 10.23960/jsl.v10i3.550

Jayaprakash, J., Srinivasan, N., and Chandrasekaran, P. 2014. Surface Modifications of CuO Nanoparticles using Ethylene Diamine Tetra Acetic Acid as a Capping Agent by Sol-Gel Routine. *Spectrochimica Acta - Part A: Molecular and Biomolecular Spectroscopy* 123: 363–368. DOI: 10.1016/j.saa.2013.12.080

Khan, I., Saeed, K., and Khan, I. 2019. Nanoparticles: Properties, Applications and Toxicities. *Arabian Journal of Chemistry* 12(7): 908–931. DOI: 10.1016/j.arabjc.2017.05.011

Kong, I., Ahmad, S., Abdullah, M., Hui, D., Yusof, A. N., and Puryanti, D. 2010. Magnetic and Microwave Absorbing Properties of Magnetite–Thermoplastic Natural Rubber Nanocomposites. *Journal of Magnetism and Magnetic Materials* 322(21): 3401–3409. DOI: 10.1016/j.jmmm.2010.06.036

La Mantia, F. P., and Morreale, M. 2011. Green Composites: A Brief Review. *Composites Part A: Applied Science and Manufacturing* 42(6): 579–588. DOI:

10.1016/j.compositesa.2011.01.017

Laksono, G. D., Rahayu, I. S., Karlinasari, L., Darmawan, W., and Prihatini, E. 2023. Characteristics of Magnetic Sengon Wood Impregnated with Nano Fe_3O_4 and Furfuryl Alcohol. *Journal of the Korean Wood Science and Technology* 51(1): 1–13. DOI: 10.5658/wood.2023.51.1.1

Liu, T. T., Cao, M. Q., Fang, Y. S., Zhu, Y. H., and Cao, M. S. 2022. Green Building Materials Lit Up by Electromagnetic Absorption Function: A Review. *Journal of Materials Science and Technology* 112: 329–344. DOI: 10.1016/j.jmst.2021.10.022

Lou, X. W., Archer, L. A., and Yang, Z. 2008. Hollow Micro-/Nanostructures: Synthesis and Applications. *Advanced Materials* 20(21): 3987–4019. DOI: 10.1002/adma.200800854

Lou, Z., Han, H., Zhou, M., Han, J., Cai, J., Huang, C., Zou, J., Zhou, X., Zhou, H., and Sun, Z. 2018. Synthesis of Magnetic Wood with Excellent and Tunable Electromagnetic Wave-Absorbing Properties by a Facile Vacuum/Pressure Impregnation Method. *ACS Sustainable Chemistry and Engineering* 6(1): 1000–1008. DOI: 10.1021/acssuschemeng.7b03332

Lumen, L., and OpenStax. 2021. *Fundamentals of Heat, Light and Sound*. NSCC, Dartmouth.

Magdalena, A. G., Silva, I. M. B., Marques, R. F. C., Pipi, A. R. F., Lisboa-Filho, P. N., and Jafelicci, M. 2018. EDTA-Functionalized Fe_3O_4 Nanoparticles. *Journal of Physics and Chemistry of Solids* 113: 5–10. DOI: 10.1016/j.jpcs.2017.10.002

Mania, P., Wróblewski, M., Wójciak, A., Roszyk, E., and Molinski, W. 2020. Hardness of Densified Wood in Relation to Changed Chemical Composition. *Forests* 11(506): 1–12. DOI: 10.3390/f11050506

Marques, P. A., Trindade, T., and Neto, C. P. 2006. Titanium Dioxide/Cellulose Nanocomposites Prepared by a Controlled Hydrolysis Method. *Composites Science and Technology* 66(7–8): 1038–1044. DOI: 10.1016/j.compscitech.2005.07.029

Martawijaya, A., Hadjodarsono, S., and Haji, M. 2005. *Atlas Kayu Indonesia Jilid II*. Pusat Penelitian dan Pengembangan Hutan dan Konservasi Alam, Bogor. DOI: 10.1163/22941932-90001149

Martins, L. C., Silva, C. S., Fernandes, L. C., Sampaio, Á. M., and Pontes, A. J. 2023. Evaluating the Electromagnetic Shielding of Continuous Carbon Fiber Parts Produced by Additive Manufacturing. *Polymers* 15(24): 4649. DOI: 10.3390/polym15244649

Masoudi, A., Hosseini, H. R. M., Shokrgozar, M. A., Ahmadi, R., and Oghabian, M. A. 2012. The Effect of Poly (Ethylene Glycol) Coating on Colloidal Stability of Superparamagnetic Iron Oxide Nanoparticles as Potential MRI Contrast Agent. *International Journal of Pharmaceutics* 433(1–2): 129–141. DOI: 10.1016/j.ijpharm.2012.04.080

Merk, V., Chanana, M., Gierlinger, N., Hirt, A. M., and Burgert, I. 2014. Hybrid Wood Materials with Magnetic Anisotropy Dictated by the Hierarchical Cell Structure. *ACS Applied Materials and Interfaces* 6(12): 9760–9767. DOI: 10.1021/am5021793

Muflihati, M., Nawawi, D. S., Rahayu, I. S., and Syafii, W. 2014. The Color Change of Jabon Wood Stained by Bark Extract of Samak Wood (*Syzygium inophyllum*). *Jurnal Ilmu dan Teknologi Kayu Tropis* 12(1): 11–19. DOI: 10.51850/jitkt.v12i1.78.g75

Oka, H., and Fujita, H. 1999. Experimental Study on Magnetic and Heating Characteristics of Magnetic Wood. *Journal of Applied Physics* 85: 5732–5734. DOI: 10.1063/1.370267

Oka, H., Terui, M., Osada, H., Sekino, N., Namizaki, Y., Oka, H., and Dawson, F. P. 2012. Electromagnetic Wave Absorption Characteristics Adjustment Method of Recycled Powder-Type Magnetic Wood for Use as a Building Material. *IEEE Transactions on Magnetics*

48(11): 3498–3500. DOI: 10.1109/tmag.2012.2196026

Peternele, W. S., Fuentes, V. M., Fascineli, M. L., Silva, J. R. D., Silva, R. C., Lucci, C. M., and Azevedo, R. B. D. 2014. Experimental Investigation of the Coprecipitation Method: An Approach to Obtain Magnetite and Maghemite Nanoparticles with Improved Properties. *Journal of Nanomaterials* 2014: 682985. DOI: 10.1155/2014/682985

Prihatini, E., Wahyuningtyas, I., Rahayu, I., and Ismail, R. 2022. Modification of Fast-Growing Wood into Magnetic Wood with Impregnation Method Using Fe_3O_4 Nanoparticles. *Jurnal Sylva Lestari* 10(2): 211–222. DOI: 10.23960/jsl.v11i2.651

Prihatini, E., Wahyuningtyas, I., Rahayu, I. S., and Ismail, R. 2023. Pengaruh Larutan Furfuril Alkohol dan Nanopartikel SiO_2 pada Beberapa Metode Impregnasi Kayu Jabon. *Indonesian Journal of Laboratory* 6: 7–13. DOI: 10.22146/ijl.v0i3.84108

Rahayu, I., Pratama, A., Darmawan, W., Nandika, D., and Prihatini, E. 2021. Characteristics of Impregnated Wood by Nano Silica from Betung Bamboo Leaves. *IOP Conf. Series: Earth and Environmental Science* 891(1): 012019. DOI: 10.1088/1755-1315/891/1/012019

Rahayu, I., Prihatini, E., Ismail, R., Darmawan, W., Karlinasari, L., and Laksono, G. D. 2022. Fast-Growing Magnetic Wood Synthesis by an In-Situ Method. *Polymers* 14(11): 2137. DOI: 10.3390/polym14112137

Rahayu, I., Zaini, L., Nandika, D., Darmawan, W., Prihatini, E., and Agustian, R. 2020. Physical Properties of Impregnated Sengon Wood by Monoethylen Glycol and Nano Silica from Betung Bamboo Sticks. *IOP Conference Series: Materials Science and Engineering* 935(1). DOI: 10.1088/1757-899x/935/1/012057

Sandberg, D., Kutnar, A., and Mantanis, G. 2017. Wood Modification Technologies - A Review. *iForest - Biogeosciences and Forestry* 10(6): 895–908. DOI: 10.3832/ifor2380-010

Schwertmann, U., Cornell, R. M., Rao, C. N. R., Raveau, B., Jolivet, J. P., Henry, M., and Livage, J. 2003. *The Iron Oxides: Structure, Properties, Reactions, Occurrences and Uses (Second)*. Wiley-VCH, Weinheim. DOI: 10.1002/3527602097

Silvia, L., Aslama, B., Novialent, E., and Zainuri, M. 2021. Synthesis of Magnetite Fe_3O_4 from Laterite Iron Rock as Microwave Absorber Material. *Journal of Physics: Conference Series* 1951: 012024. DOI: 10.1088/1742-6596/1951/1/012024

Sompech, S., Srion, A., and Nuntiya, A. 2012. The Effect of Ultrasonic Treatment on the Particle Size and Specific Surface Area of $LaCoO_3$. *Procedia Engineering* 32: 1012–1018. DOI: 10.1016/j.proeng.2012.02.047

Sopacua, F., Wijayanto, N., and Wirnas, D. 2021. Growth of Three Types of Sengon (*Paraserianthes* spp.) in Varying Planting Spaces in Agroforestry System. *Biodiversitas* 22(10): 4423–4430. DOI: 10.13057/biodiv/d221035

Suri, I. F., Purusatama, B. D., Kim, J. H., Hidayat, W., Hwang, W. J., Iswanto, A. H., Park, S. Y., Lee, S. H., and Kim, N. H. 2023. Durability of Heat-Treated *Paulownia tomentosa* and *Pinus koraiensis* Woods in Palm Oil and Air against Brown- and White-Rot Fungi. *Scientific Reports* 13: 21929. DOI: 10.1038/s41598-023-48971-z

Teng, T. J., Arip, M. N. M., Sudesh, K., Nemoikina, A., Jalaludin, Z., Ng, E. P., and Lee, H. L. 2018. Conventional Technology and Nanotechnology in Wood Preservation: A Review. *BioResources* 13(4): 9220–9252. DOI: 10.15376/biores.13.4.teng

Theerdhala, S., Bahadur, D., Vitta, S., Perkas, N., Zhong, Z., and Gedanken, A. 2010. Sonochemical Stabilization of Ultrafine Colloidal Biocompatible Magnetite Nanoparticles Using Amino Acid, L-Arginine, for Possible Bio Applications. *Ultrasonics Sonochemistry*

17(4): 730–737. DOI: 10.1016/j.ultsonch.2009.12.007

Trey, S., Olsson, R. T., Ström, V., Berglund, L., and Johansson, M. 2014. Controlled Deposition of Magnetic Particles Within the 3-D Template of Wood: Making Use of the Natural Hierarchical Structure of Wood. *RSC Advances* 4(67): 35678–35685. DOI: 10.1039/c4ra04715j

Tukan, D. N., Rosmainar, L., Kustomo, K., and Rasidah, R. 2023. A Review: Optimum Conditions for Magnetite Synthesis (Fe_3O_4). *Jurnal Berkala Ilmiah Sains dan Terapan Kimia* 17(2): 15. DOI: 10.20527/jstk.v17i2.15134

Wahyuningtyas, I., Rahayu, I. S., Maddu, A., and Prihatini, E. 2022. Magnetic Properties of Wood Treated with Nano-Magnetite and Furfuryl Alcohol Impregnation. *BioResources* 17(4): 6496–6510. DOI: 10.15376/biores.17.4.6496-6510

Wang, M., Wang, N., Tang, H., Cao, M., She, Y., and Zhu, L. 2012. Surface Modification of Nano-Fe_3O_4 with EDTA and its Use in H_2O_2 Activation for Removing Organic Pollutants. *Catalysis Science and Technology* 2(1): 187–194. DOI: 10.1039/c1cy00260k

Wardiyati, S., Adi, W. A., and Winatapura, S. 2018. Sintesis dan Karakterisasi Microwave Absorbing Material Berbasis Ni-SiO_2 dengan Metode Sol-Gel. *Jurnal Fisika* 8(2): 51–59. DOI: 10.15294/jf.v8i2.16975

Xu, H., Bi, H., Yang, R., Xu, H., Bi, H., and Yang, R. 2013. Enhanced Microwave Absorption Property of Bowl-Like Fe_3O_4 Hollow Spheres/Reduced Graphene Oxide Composites Enhanced Microwave Absorption Property of Bowl-Like Fe_3O_4 Hollow Spheres/Reduced Graphene Oxide Composites. 522(2012): 2012–2015. DOI: 10.1063/1.3691527

Zakaria, Z., Sattar, S., and Zulkifli, S. A. 2021. *Advances in Electrical and Electronic Engineering and Computer Science*. Springer Singapore, The Gateway. DOI: 10.1007/978-981-33-6490-5

Zheng, D., Dong, R., Li, Q., and Qiu, X. 2021. Investigation on the Binding Force Between Lignin and Magnetic Fe_3O_4 Nanoparticles with AFM. *Applied Surface Science* 538: 148146. DOI: 10.1016/j.apsusc.2020.148146